

Biomineralization in Cement and Concrete Research

Nicolas D. Dowdy ^{a, #} *and Wil V. Sru bar III* ^{a, b, *}

^a Materials Science and Engineering Program, University of Colorado Boulder, 4001 Discovery Drive, UCB 027, Boulder, Colorado USA 80303. ^b Department of Civil, Environmental, and Architectural Engineering, University of Colorado Boulder, 1111 Engineering Drive ECOT 441

UCB 428, Boulder, Colorado USA 80309. #Lead Author: nicolas.dowdy@colorado.edu;

*Corresponding Author: wsrubar@colorado.edu

Abstract: Biominerization refers to the biological processes through which living organisms produce minerals. In recent years, biominerizing microorganisms have been used to stabilize soil or to impart a self-healing or self-sealing mechanism to damaged cement and concrete materials. However, applications of biominerals in cement and concrete research can extend far beyond these applications. This article focuses on the biominerization of calcium carbonate (CaCO_3) and silicon dioxide (SiO_2) and their past, present, and future potential applications in cement and concrete research. First, we review the mechanisms of CaCO_3 and SiO_2 biominerization and the micro- and macroorganisms involved in their production. Second, we showcase the wide array of biomineral architectures, with an explicit focus on CaCO_3 polymorphs and SiO_2 morphologies found in nature. Third, we briefly summarize previous applications of CaCO_3 and SiO_2 biominerization in cement and concrete research. Finally, we discuss emerging applications of biominerals in cement and concrete research, including mineral admixtures or raw meal for portland cement production, as well as other applications that extend beyond self-healing.

Keywords: Biomineralization; cement; concrete; calcium carbonate (CaCO_3); silicon dioxide (SiO_2).

26 **1.0 Introduction**

27 Biominerization is the biological process by which living organisms produce minerals. By mass,
28 calcium carbonate (CaCO_3) is the most abundant biomineral found in nature [1]. Microorganisms,
29 such as bacteria [2], fungi [3], and coccolithophores [4], and macroorganisms, such as mollusks
30 [5] and coral [6], are well known to biomineralize CaCO_3 . The biominerization of silicon dioxide
31 (*i.e.*, silica) (SiO_2) [7–10], calcium phosphate (*i.e.*, apatite) [11,12], magnesium hydroxide (*i.e.*,
32 brucite) (Mg(OH)_2) [13–15], iron oxides (*e.g.*, hematite, magnetite) (Fe_2O_3) [16,17], and
33 aluminum oxide (*i.e.*, alumina) (Al_2O_3) [7,18,19] also occurs in a multitude of micro- and
34 macroorganisms, such as diatoms [9], bacteria [17], mollusks [5] and other higher-level organisms
35 [20–23].

36 CaCO_3 and SiO_2 biominerization has been applied in select applications relevant to the
37 field of cement and concrete research. These areas include soil stabilization [24], beneficiation of
38 recycled concrete aggregates [25] and recycled plastic aggregates [26], living building materials
39 [27], and self-healing [2,28] or self-sealing [29,30] concrete. While most applications concern
40 CaCO_3 biominerization, one study [31] recently showed that biomineralized SiO_2 from diatoms
41 exhibit moderate to high pozzolanic reactivity, indicating their suitability as a supplementary
42 cementitious material (SCM). Despite the prevalence of CaCO_3 and SiO_2 biominerization in
43 nature, the applications of biominerization in cement and concrete research are predominantly
44 limited to these few examples.

45 In this work, we elucidate how biominerization can be leveraged to further the
46 development of sustainable and resilient cementitious materials. First, we outline the main
47 mechanisms of biominerization, with a focus on the two most common biominerals produced by
48 living organisms, CaCO_3 and SiO_2 . Second, we showcase the wide variety of CaCO_3 polymorphs
49 and SiO_2 morphologies and discuss the potential for their physical and chemical tunability. Finally,
50 we highlight past examples and future opportunities for direct applications of these materials in
51 cement and concrete research. Lastly, we highlight the challenges that will need to be addressed to
52 translate biominerization technologies from the benchtop to a commercially viable scale.

53

54 **2.0 Mechanisms of CaCO_3 and SiO_2 Biominerization**

55 **2.1 CaCO_3 Biominerization**

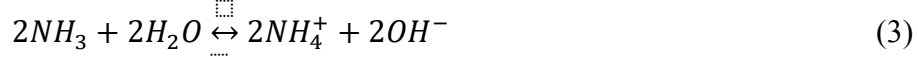
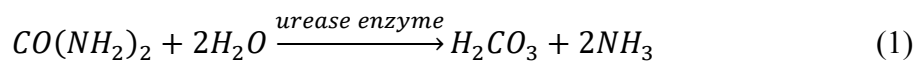
56 CaCO_3 biominerization is mediated by the metabolic activity of micro- and macroorganisms. In
57 this section, we review four of the most common mechanisms of CaCO_3 mineralization: urea
58 hydrolysis, photosynthesis, sulfate reduction, and protein-mediated biominerization. Most
59 involve the production of carbonic acid, which is further decomposed into the bicarbonate anion
60 (HCO_3^{2-}) that can subsequently react with free calcium (Ca^{2+}) if it is present in the surrounding
61 media. The result is the formation of biologically architected CaCO_3 with properties that can be
62 tuned by tailoring the mineralization kinetics *via* controlling the metabolic activities of the
63 organism [32,33].

64

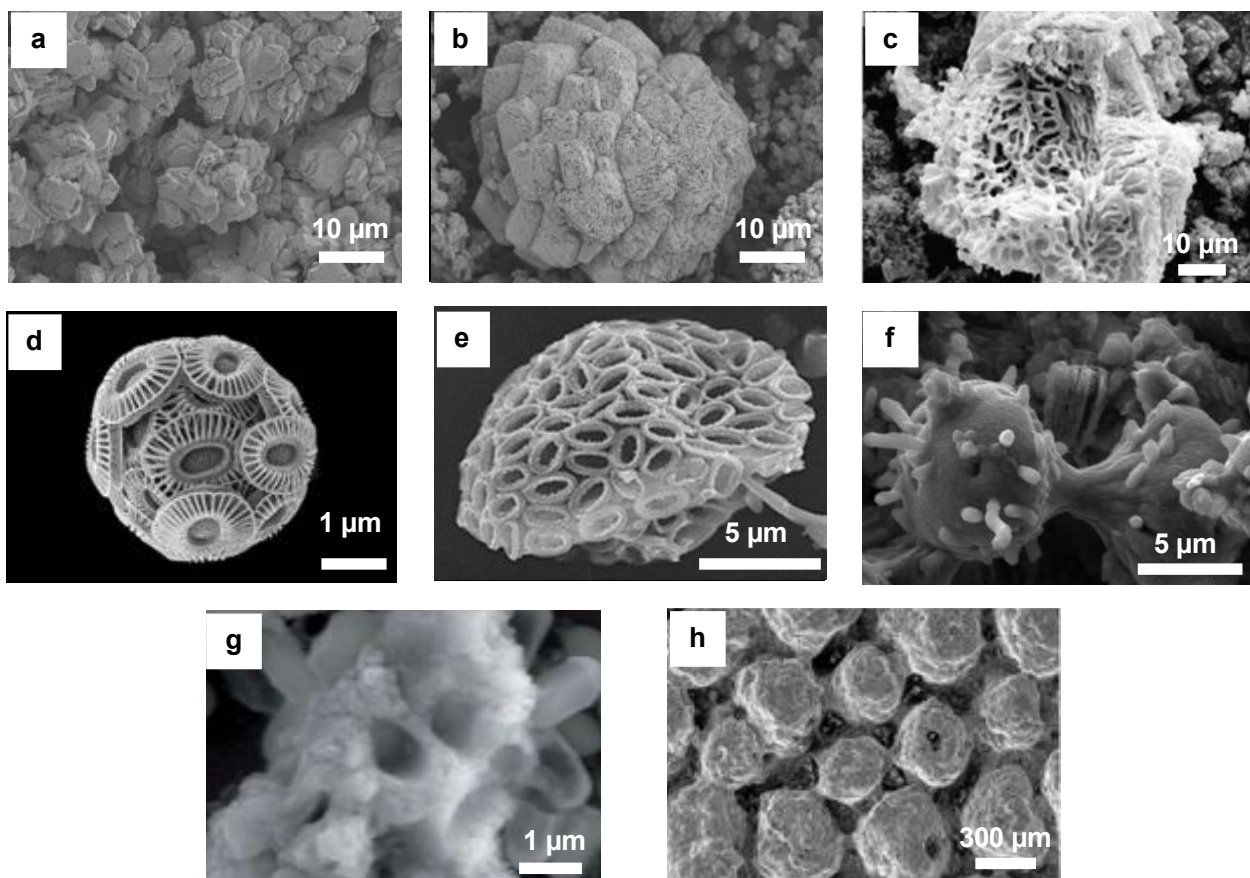
65 **2.1.1 Urea hydrolysis**

66 The urea hydrolysis mechanism of CaCO_3 biominerization is well understood [3,34–37]. CaCO_3
67 biominerization *via* urea hydrolysis is a vital process for bacteria, such as *Sporosarcina pasteurii*
68 [38], and fungi, such as *Fusarium cerealis* [3]. These organisms employ urea hydrolysis to break
69 down urea so that it may be consumed as a carbon source in exchange for energy. These organisms
70 can biomineralize and produce CaCO_3 if Ca^{2+} ions are present in the media. Without Ca^{2+} ,
71 however, these organisms will not biomineralize.

72 The urea hydrolysis mechanism of CaCO_3 biomineralization is as follows:
73



80 The biomineralization reaction is catalyzed by the metabolic production of the urease enzyme. In
81 the presence of urea, urease will catalyze the decomposition of urea into carbonic acid and
82 ammonia. The carbonic acid will subsequently dissociate into bicarbonate and hydrogen ions,
83 which lowers the pH. However, the ammonia will react with water to form ammonium and
84 hydroxide ions, which increases the pH. The hydroxide and bicarbonate anions then react to form
85 carbonate anions and water. The former can react with free Ca^{2+} to yield precipitated CaCO_3 .
86 Images of biomineralized CaCO_3 through urea hydrolysis are shown in **Figure 1(a)-(c)**.
87



88
89
90 **Figure 1.** Biomineralized CaCO_3 produced via (a-c) urea hydrolysis [(a) *S. pasteurii* (Heveran et
91 al. [32], CC BY 4.0) (b) *Escherichia coli* (Heveran et al. [32], CC BY 4.0), (c) *Bacillus latus* (Wei
92 et al. [39], CC-BY-NC), (d-e) photosynthesis [(d) *Emiliania huxleyi* (Neukermans et al. [40], CC-
93 BY), (e) *Pleurochrysis dentata* (Chen et al. [41], CC-BY-4.0), (f) sulfate reduction [*Desulfovibrio*

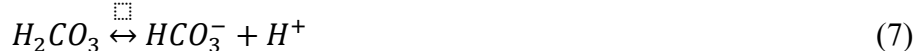
94 *bizertensis* (Lin et al. [42], copyright 2018 Elsevier), and (g-h) protein-mediated biomineralization
95 [(g) bacterial precipitation *Bacillus subtilis* (Liu et al.[43], (h) *Sphaerotilus erbeni* eggshells
96 (Grellet-Tinner et al. [44] copyright 2012 SEPM).

97 From a cement and concrete research perspective, advantages of CaCO_3 biomineralization *via* urea
98 hydrolysis include the autonomous production of higher quantities of biomineralized CaCO_3
99 compared to other CaCO_3 biomineralization mechanisms on a per-volume basis (e.g., 1.6-9.8 mg/L
100 from ureolysis [45] compared to 0.8-2.2 mg/mL from photosynthesis [46]). In addition, the high-
101 pH tolerance of spore-forming, biomineralizing microorganism species (e.g., *Bacillus sphaericus*,
102 *Phoma herbarum*, *Bacillus subtilis*, *Sporosarcina pasteurii*) [2,3] are a notable advantage, given
103 the high pH of the pore solution within hydrated cement paste. However, disadvantages of urea
104 hydrolysis include the production of ammonia and ammonium as byproducts of CaCO_3
105 biomineralization and the need to add an exogenous source of Ca^{2+} (e.g., CaCl_2) to the media,
106 which can then lead to the addition of undesirable byproducts (e.g., chloride anions) to the
107 cementitious matrix [38]. In addition, the cost and availability of urea-rich media has been noted
108 as another significant challenge impeding widespread adoption. Nevertheless, CaCO_3
109 biomineralization *via* urea hydrolysis has been widely employed in cement and concrete research
110 because of the potential benefits that CaCO_3 biomineralization can impart to cementitious
111 materials (see **Section 4**).

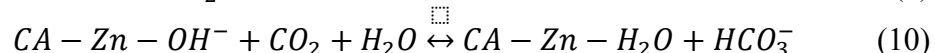
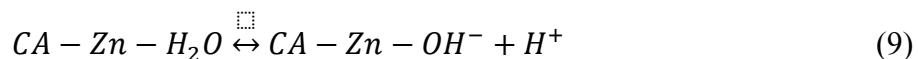
112 2.1.2 Photosynthesis

113 By definition, photosynthesis is the metabolic process by which organisms produce energy and
114 mass *via* biochemical reactions involving light and carbon dioxide (CO_2) [47]. Photosynthetic
115 microorganisms, including certain strains of cyanobacteria [48] and phytoplankton (e.g.,
116 coccolithophores) [4], and macroorganisms, such as calcareous macroalgae [49], produce CaCO_3
117 through photosynthesis-driven biomineralization. Coccolithophores alone are responsible for
118 sequestering and storing $\sim 1.5\text{-}5.9 \text{ GtCO}_2/\text{year}$ ($\sim 0.4\text{-}1.6 \text{ GtC/year}$) as biomineralized CaCO_3 [50],
119 which equates to $\sim 3.4\text{-}13.4 \text{ Gt CaCO}_3$. Photosynthesis-driven CaCO_3 biomineralization is
120 mediated by the production of carbonic anhydrase (CA), an enzyme that catalyzes the rapid
121 conversion of CO_2 into carbonic acid [51].

122 The photosynthesis mechanism of CaCO_3 biomineralization is as follows:



123 While these reactions represent the most prominent pathway for photosynthesis-driven CaCO_3
124 biomineralization [47], carbonic anhydrase (CA) is known to facilitate other CaCO_3
125 biomineralization pathways in which it forms metal complexes with zinc (Zn^{2+}) and Ca^{2+} to yield
126 bicarbonate and, ultimately, biomineralized CaCO_3 [52]:



138

139 Photosynthesis-driven CaCO_3 biomineralization has two distinct advantages. First, the economics
140 of CaCO_3 biomineralization *via* photosynthesis are advantageous. Most photosynthetic species
141 that biomineralize CaCO_3 are marine micro- and macroorganisms, which require only sunlight,
142 seawater, and CO_2 . Second, photosynthesis-driven CaCO_3 biomineralization is a form of direct
143 CO_2 capture and storage. CO_2 dissolves into the media with assistance from carbonic anhydrase.
144 This CO_2 is converted to inorganic biominerals (*i.e.*, CaCO_3) and organic molecules (*e.g.*, lipids,
145 proteins, carbohydrates) that comprise the micro- and macroorganism cell bodies. Disadvantages
146 of CaCO_3 biomineralization *via* photosynthesis include lower quantities of biominerals per volume
147 basis and the pH sensitivity of biomineralizing strains of photosynthetic microorganisms, which
148 makes them less suitable for direct incorporation into concrete mixtures. Instead, researchers have
149 found other means to leverage photosynthesis-driven biomineralization. For example, Murphy *et*
150 *al.*, explored the use of CaCO_3 derived from coccolithophores, which are biomineralizing
151 photosynthetic microalgae, as a nucleating agent in portland limestone cement (PLC) paste [53].
152 Researchers have also used photosynthesis-driven biomineralization to produce enzymatic [54] or
153 living building materials [31] (see **Section 4**). Images of biomineralized CaCO_3 through
154 photosynthesis are also shown in **Figure 1(d)-(e)**.

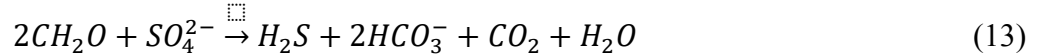
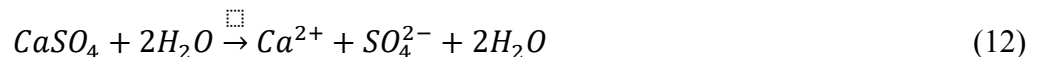
155

156 2.1.3 Sulfate Reduction

157 Sulfate reduction is an intermediate step for energy production in some species of anaerobic
158 bacteria, including *Desulfovibrio bizertensis* [55] and *Desulfomicrobium baculum* [56]. While
159 biomineralization *via* sulfate reduction is less studied than urea hydrolysis or photosynthesis, the
160 mechanism of biomineralization is similar in that the formation of carbonic acid is key from a
161 biochemical standpoint.

162 There are two sulfate reduction mechanisms of CaCO_3 biomineralization. The first
163 involves the dissociation of calcium sulfate, where the cell produces formaldehyde (*i.e.*, CH_2O)
164 and converts it to sulfuric acid (H_2S), bicarbonate, CO_2 and water as part of the intermediate step
165 [47,57,58]:

166

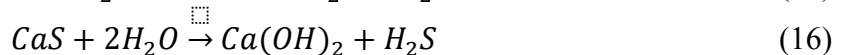
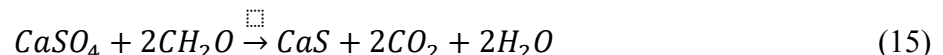


170

171 Sulfate reducing organisms require an exogenous source of calcium sulfate in the medium to
172 nucleate an external layer of CaCO_3 directly on its cell membrane, which then leads to subsequent
173 precipitation and growth of CaCO_3 from the medium onto the cell-templated CaCO_3 [22].

174 The second mechanism is similar to the first, except that it involves the metabolic
175 production of calcium sulfate rather than relying on an external source:

176



181 In terms of its utility, sulfate reduction is less advantageous than urea hydrolysis or photosynthesis
182 because it necessitates the production of formaldehyde and H₂S. Additionally, sulfate reduction
183 has limited potential in self-healing concrete applications because the reaction itself decreases the
184 pH [59]. Interestingly, some sulfate-reducing organisms can be found in highly alkaline
185 environments [59,60], which is why the mechanism could still be investigated for different cement
186 and concrete applications in which the H₂S can be captured or toxicity is not an issue. An example
187 of CaCO₃ biomineralized *via* sulfate reduction is shown in **Figure 1(f)**.
188

189 2.1.4 Protein-mediated

190 Protein-mediated CaCO₃ biomineralization is observed in mollusks, crustaceans, and avian eggs
191 [61]. In protein-mediated biomineralization, surface proteins, such as those rich in arginine [62]
192 act as positively charged nucleation sites that facilitate the interactions between CO₃²⁻ and Ca²⁺
193 present in the surrounding media. The proteins seed amorphous CaCO₃ (ACC) minerals that
194 precipitate and grow into larger CaCO₃ minerals comprised of ACC or one of the other polymorphs
195 of CaCO₃ (*i.e.*, calcite, aragonite, vaterite) (see **Section 3**). This mechanism has a few distinct
196 advantages in that (1) biomineralizing microorganisms that leverage protein-mediated CaCO₃
197 biomineralization can produce larger quantities of CaCO₃ and (2) the kinetics of mineralization
198 and the resultant biomineral architectures could theoretically be tailored by modulating the
199 expression of surface proteins. However, the macroorganisms that leverage this mechanism in
200 nature have a long growth cycle, resulting in limited quantities unless large farms or naturally
201 occurring deposits can overcome such a limitation. In addition, protein-mediated CaCO₃ formation
202 *ex vivo* is less characterized when compared to the three prior mechanisms (ureolysis,
203 photosynthesis, and sulfate reduction), where the specific sequence and compounds are less well
204 defined due to the sheer number and variability of protein properties in nature. There is significant
205 work ongoing to define precise mechanistic steps [63-65], which is promising for applying these
206 principles on a larger scale in the future. **Figure 1(g)-(h)** show images of protein-mediated CaCO₃
207 biomineralization.
208

209 2.2 SiO₂ Biominerization

210 SiO₂ biominerization is an integral structure-forming process in sea sponges and diatoms [9,66]
211 (see **Figure 2**). While the biochemical mechanisms of silica biominerization are not fully
212 understood at the time of writing [9,67], studies of sea sponges and diatoms have elucidated that
213 the presence of silicic acid in the media is critical for SiO₂ mineralization. Sponges use silicateins
214 (*i.e.*, silica-rich proteins) to template and mineralize silicic acid into spicule structures in a process
215 akin to protein-mediated CaCO₃ biominerization [5,66]. However, the exact SiO₂
216 biominerization mechanism in sea sponges is still under investigation [66,68]. On the other hand,
217 SiO₂ biominerization in diatoms is better understood. Diatoms concentrate silicic acid into silica
218 pools internal to the diatom. The accumulation of silicic acid results in the polycondensation and
219 eventual precipitation of amorphous SiO₂. This precipitation of SiO₂ is aided by polyamines and
220 polysilaffins within the cell. It is hypothesized that the occurrence of positively charged functional
221 groups in both polymers attracts negatively charged silica anions to create the pools, thereby
222 facilitating polycondensation [9,67]. The precipitated SiO₂ forms the basis of the intricate
223 microporous exoskeletons that are characteristic of most diatom species (see **Figure 2c**).
224

225

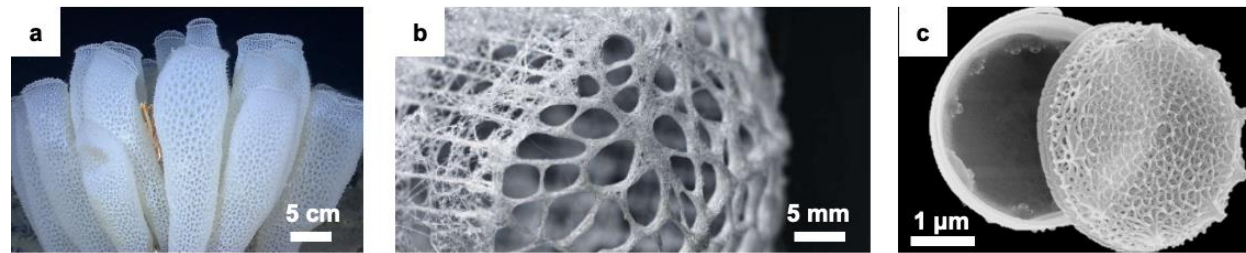


Figure 2. SiO_2 biomineralization in sea sponge *Euplectella aspergillum* at (a) centimeter scale (Imbler [69], within permissions by NOAA) and (b) millimeter scale (Monn [70], CC-BY-ND), and (c) the diatom species *Thalassiosira pseudonana* (Piccinetti et al. [71] CC-BY-4.0).

In terms of advantages, most microorganisms that biominerlize SiO_2 are photosynthetic and found in marine environments, which minimizes their media and growth requirements to sunlight, seawater, and CO_2 , along with trace nutrients. In fact, diatoms alone are responsible for $\sim 20\%$ of photosynthetically fixed CO_2 on Earth [72]. Diatoms are relatively resilient, and some species exhibit fast growth rates compared to others. Additionally, diatoms have been shown to incorporate a variety of other metal ions, including aluminum [73], magnesium [14], and zinc [74], into their biominerl architecture, which suggests an ability to tune their chemical composition. Their structures are also highly amorphous, which makes them more reactive than other silicates (e.g., clays) that may require calcination to increase reactivity. Some disadvantages include the slow growth of some species capable of SiO_2 mineralization (e.g., sponges), along with the relatively low cell densities of diatoms, particularly when compared to other microorganisms [75].

244 3.0 CaCO_3 and SiO_2 Biominerl Architectures

245 3.1 CaCO_3 Biominerl Architectures

246 Biominerlized CaCO_3 can form as one of four polymorphs: calcite, aragonite, vaterite, or ACC
247 (see **Figure 3**). Natural limestone deposits, ancient pelagic (*i.e.*, marine) sediments, are mainly
248 composed of calcite and aragonite [76]. Calcite and aragonite are more thermodynamically stable
249 than vaterite and ACC at ambient temperatures and pressures. Biologically precipitated vaterite
250 has been shown to transition to a more stable phase (*i.e.*, calcite, aragonite) over time [77]. This
251 transformation is known to take place in a matter of 10-20 hours in DI water [78], and the
252 biological systems have been shown to facilitate the increase Mg ions in solution [77], which is
253 known to stabilize aragonite and vaterite in solution [78]. ACC is most commonly found *in vivo*
254 and tends to be thermodynamically unstable *ex vivo* [79]. Understanding the differences in these
255 polymorphs is of particular interest due to their differences in physical and chemical stability and
256 how that stability can affect cement hydration and strength when different CaCO_3 particles are
257 added to a cementitious system [80].

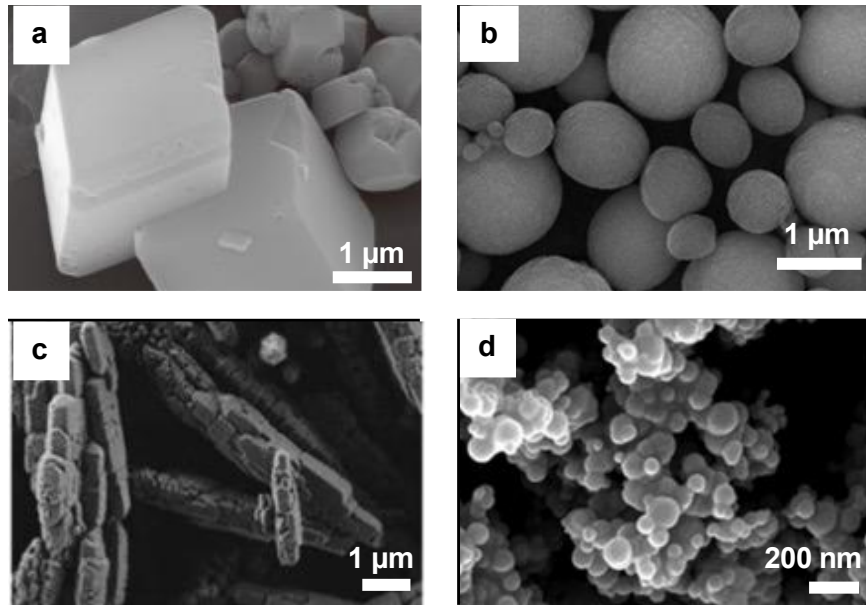
226
227

228
229
230
231

232
233
234
235
236
237
238
239
240
241
242
243

244
245

246
247
248
249
250
251
252
253
254
255
256
257
258



259
260
261 **Figure 3.** Morphologies of (a) calcite (Yang et al. [81], CC BY 4.0), (b) vaterite (Gilad et al. [82],
262 CC BY NC 3.0), (c) aragonite (Myszka et al. [83], CC BY NC 3.0), and (d) amorphous calcium
263 carbonate (ACC) (Xto et al. [84], CC BY 4.0).

264
265 Calcite, the most stable CaCO_3 polymorph, is characterized by its rhombohedral microstructure
266 [85]. Calcite is known to be biomineralized by bacteria [2], algae [86], fungi [3], and sponges [87].
267 Nanoscale biomineralized calcite crystals can form aggregates up to 200 μm , but the size depends
268 on the conditions within the cells and the size of the cell itself [32,42,53,88]. Coccolithophores
269 form individual coccoliths comprised mostly of calcite that can be much smaller in size (*i.e.*, 1-4
270 μm) [53,86,89]. Researchers have shown that individual coccolithophore species and growth
271 conditions, including temperature, pH, and CO_2 exposure [89], have a significant effect on
272 coccolith formation.

273 Aragonite, the second most stable polymorph of CaCO_3 , is characterized by its orthorhombic
274 crystal structure [90]. Aragonite can be found in nature alongside calcite. Aragonite is known to
275 be biomineralized by coral [6] and mollusks. [5,91]. Nacre is an example of biomineralized
276 aragonite layered in a lamellar structure with a protein matrix. The proteins provide a scaffold for
277 aragonite nucleation, while the aragonite provides strength to the nacre [5]. When precipitated in
278 solution at ambient temperatures, aragonite has a tendency to redissolve into solution and
279 precipitate as calcite [90,92], but aragonite is stable enough to exist on its own at ambient
280 temperatures and pressures.

281 In comparison to calcite and aragonite, vaterite is the least stable crystalline polymorph.
282 Vaterite is biomineralized by fish [93], ascidians [94], snails, and bacteria [93,95–97]. Pure vaterite
283 will dissolve in water and reprecipitate as calcite at ambient temperatures or vaterite at elevated
284 temperatures through a dissolution-precipitation reaction. The instability (*i.e.*, water solubility) of
285 vaterite has been leveraged for applications that require readily soluble CaCO_3 [98]. From a cement
286 and concrete research perspective, vaterite has been shown to precipitate, along with calcite and
287 aragonite, in self-healing concrete applications [99].

288 ACC is the least stable CaCO_3 polymorph. ACC is generally a precursor to other forms of
289 biomineralized CaCO_3 [77,79,84] in which it is precipitated and temporarily stabilized before it

transforms into a more stable polymorph. ACC has been shown to be stabilized by organic molecules *ex situ* [88] and can exist as stable intracellular structures (or inclusions) *in situ* in some prokaryotes [100]. However, the exact mechanisms of its initial formation and stability remain under investigation [84,100]. Evidence of ACC biomineralization was first found in eukaryotic organisms [79]. ACC has also been identified in prokaryotic organisms [100]. In biological systems, ACC provides a number of functions, such as scaffolding for tissues and even influence the short-range crystalline order of crystalline polymorphs of CaCO_3 [101], most particularly of calcite and aragonite [102].

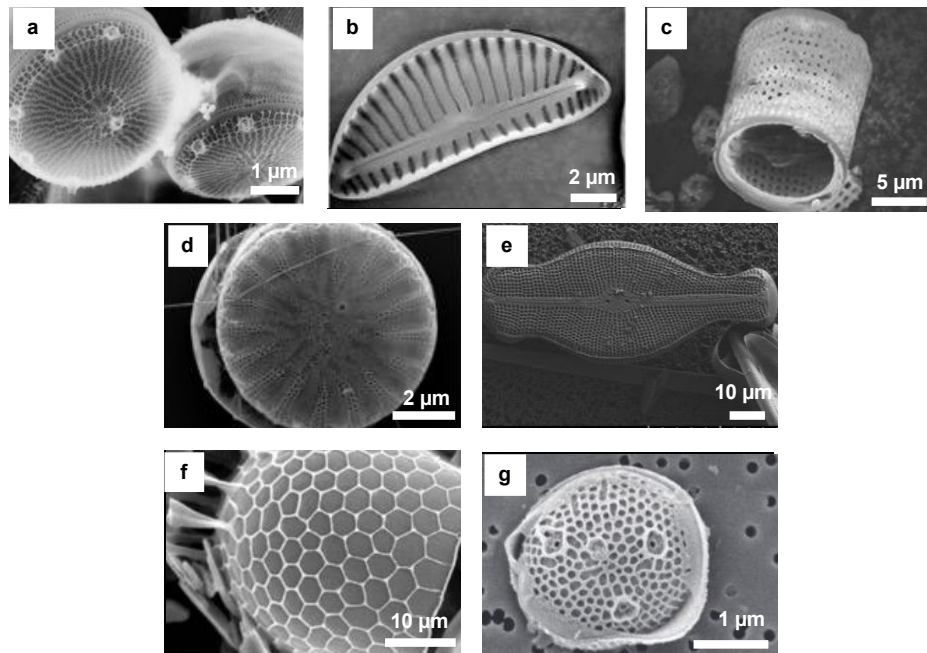
298

299 **3.2 SiO_2 Biomineral Architectures**

300 In terms of morphological features, SiO_2 forms spicules, as with sea sponges, or frustules, as with 301 diatoms. Sea sponges use SiO_2 to build these spicules to make up their skeletons, which exhibit 302 different structural features throughout their cross-section [103]. These spicules are visible on the 303 macroscale as tree-like growths that branch upwards and away from the base of the seafloor [66]. 304 At the microscale, these spicules are composed of long, cylindrical spines, which are generally 305 made of micrometer-scale sheets stacked on top of each other [104]. The spicules are typically 306 composed of semi-crystalline filaments, which contain crystalline and amorphous SiO_2 and 307 crystallized protein [23]. Thus, the exact degree of crystallinity of the SiO_2 can be difficult to 308 quantify due to the crystallized proteins within the spicules [66].

309 Diatoms use SiO_2 to build their exoskeletons, or frustules. **Figure 4** illustrates the 310 morphological diversity of diatom frustules. These frustules are porous to enable the function of 311 organic valves used for transport. Diatom frustules, which are generally on the order of 312 micrometers [15,103,105], are typically composed of amorphous or semi-crystalline SiO_2 [73]. 313 Similar to sponges, this characterization is often complicated by interfering chemical components, 314 where in diatoms, this is generally in the form of incorporated and surface elements, such as 315 aluminum [7,106], iron [15], and magnesium [8,14]. The incorporation of such metals helps limit 316 the dissolution of amorphous silica in the frustule, thereby enhancing its chemical and structural 317 stability.

318



319

320

321 **Figure 4.** Morphological diversity of diatom frustules. (a) *Thalassiosira pseudonana* (Sumper et
322 al. [9], copyright 2008 Wiley-VCH), (b) *Navicula* sp. (Wang et al. [107], copyright 2012 Springer
323 Science+Business Media, LLC), (c) *Melosira* sp. (Zhang et al. [108], copyright 2011 Springer
324 Science+Business Media, LLC), (d) *Cyclotella* sp. (Rorrer et al. [109], CC BY 4.0), (e)
325 *Didymosphenia geminata* (Zglobicka et al. [110], CC BY 4.0), (f) *Chaetoceros gacilis* (Hildebrand
326 [111], copyright 2008 American Chemical Society), (g) *Minidiscus comicus* (Leblanc et al. [112],
327 CC BY 4.0).

328

329 **4.0 Applications of CaCO₃ and SiO₂ Biomineralization to Cement and Concrete Research**

330 **4.1 CaCO₃ Biomineralization Applications**

331 CaCO₃ biominerization *via* urea hydrolysis has been widely employed in cement and concrete
332 research. Ureolytic microorganisms have been applied in most self-healing [55,113,114] and self-
333 sealing [55,113] concrete applications. Ureolytic biominerization has also been shown to
334 increase the durability of concrete through porosity reduction and through the propensity of some
335 microorganisms to bind potentially harmful compounds, such as free chloride ions [2]. Recycled
336 aggregate beneficiation has also been explored using microorganisms capable of ureolytic
337 biominerization. In a seminal study conducted by Grabiec *et al.* [115], the authors found that
338 CaCO₃ biodeposition can reduce the porosity and water demand of recycled aggregates. Bakr and
339 Singh [116] demonstrated enhanced strength of cementitious systems with recycled aggregates
340 that were pre-treated with a ureolytic biominerization process. Another study examined how well
341 strains isolated from concrete aggregates performed in a similar application [117]. In addition to
342 increasing the strength of stabilized soils [24,34,113], heavy metal immobilization within soils has
343 also been enhanced through urea hydrolysis-driven biominerization [34,38,113].

344 More recently, researchers in the field of synthetic biology have shown that calcium
345 carbonate polymorphs and mechanical properties can be tailored by modulating the metabolic
346 activity of microorganisms capable of ureolytic biominerization. Heveran *et al.* demonstrated
347 how ureolytic organisms could tailor the polymorphism of CaCO₃ when using engineered strains
348 of *E. coli* [32]. These same strains were used in a subsequent study to produce biominerized
349 living building materials [118]. Other researchers have isolated the urease enzyme and used it
350 directly to enhance biominerization in soil stabilization applications in which ensuring the long-
351 term viability of the microorganisms is less feasible [38].

352 Applications of CaCO₃ biominerization *via* photosynthesis has been less explored in
353 cement and concrete research. One study conducted by Rizwan *et al.* [119] showed how the
354 introduction of photosynthetic microorganisms into cement paste systems can decrease porosity,
355 although whether these effects persist at later ages and whether the microorganisms can survive
356 long-term is largely unknown. Noting the aggressive pH environment in traditional cementitious
357 materials, some researchers are rethinking the matrix into which biominerizing microorganisms
358 are embedded. For example, in the seminal study on living building materials [120], researchers
359 used photosynthetic microorganisms capable of biominerization to strengthen and toughen a
360 sand-hydrogel scaffold. The data showed that microbial survivability within the sand-hydrogel
361 scaffold was 9% to 14% after 30 days, which exceeded previous reports on microbial survivability
362 in self-healing concrete applications (0.1% to 0.4%) for similar timeframes [32]. Murphy *et al.*
363 produced CaCO₃ using coccolithophores, biominerizing microalgae, and showed that it could
364 serve as a functional CO₂-negative CaCO₃ filler in PLC pastes [53]. Wang *et al.* [54] isolated the
365 carbonic anhydrase enzyme and used it to make an enzymatic construction material. The authors

366 used gelatin, carbonic anhydrase, calcium chloride dihydrate solution, and ambient CO₂ to
367 generate a mortar with comparable compressive strength to conventional mortars.

368 Applications of biomineralization *via* sulfate reduction are limited in comparison to
369 ureolytic biomineralization. Byrd *et al.* [121] demonstrated that biomineralization *via* sulfur
370 reduction in a citrate production process yielded a calcite-rich sediment, which could provide
371 additional benefit of improving the durability of concrete vessels in which the reactions were
372 taking place. Sulfate reduction has also been used to reduce uranium stored in concrete, which can
373 reduce the risk of corrosion induced by uranium and its associated compounds [122]. While sulfate
374 reduction has only been achieved chemically in this application, the results suggest that similar
375 results could be achieved using a biological approach. In wastewater concrete pipe applications,
376 biomimeticizing sulfur reducing microorganisms could potentially enhance concrete strength and
377 increase durability by reducing the rates of microbially induced concrete corrosion [123].
378 Protein-mediated biomimeticization in cement and concrete research has focused on studying the
379 effects of adding biomimeticized shells and protein additives into cementitious systems. For
380 example, cement replacement with eggshells have been shown to reduce the embodied carbon
381 emissions of concrete [124,125]. Ground oyster shells have been shown to reduce porosity in
382 geopolymers [126] and decrease chloride diffusion in portland cement systems [127].
383 Compressive strength has been shown to increase at an optimized level of cement substitution, but
384 the optimal percent substitution and corresponding increase in strength is source-dependent [128]
385 and likely affected by other CaCO₃ characteristics, such as particle size, surface area, chemical
386 composition, and residual organic polymer content. Oyster concrete, in which ground oyster shells
387 are used in lieu of fine and coarse aggregates, has also been explored [129]. Oyster concretes are
388 promising due to being abundant and having a long history of use as part of the more broad
389 category of tabby concrete [130]. Tabby concrete is not unlike Roman concrete. It is a type of lime-
390 pozzolan concrete in which oyster shells are calcined to form quicklime and combined with a
391 reactive, siliceous SCM. Studies have also used oyster shells as fine aggregate substitutes, but their
392 use as a coarse aggregate replacement warrants further investigation [131]. Martin *et al.* used
393 powdered milk to enhance ureolytic biomimeticization, where the powdered milk acted to increase
394 precipitation quantity and bond strength at the CaCO₃-SiO₂ interface of the sand samples utilized
395 in the study [132]. Another study by Baffoe and Ghahremaninezhad demonstrated how different
396 proteins are more or less effective in supporting biomimeticization. They showed that while
397 Albumin was able to stabilize vaterite, calcite, and aragonite on a sliding concentration, whey
398 protein showed negligible difference compared to control, which the authors attributed to
399 differences in protein surface charge and hydrophobicity of the proteins involved [133].

400 **4.2 SiO₂ Biomimeticization Applications**

401 Applications of SiO₂ biomimeticization in cement and concrete research was limited at the time of
402 writing. Sand, clays, slag, fly ash, and slag are the most dominant SiO₂ sources for applications
403 such as cement clinkering, fine aggregate, and cement replacement. Biological SiO₂ applications
404 have been limited to the use of agricultural waste (*e.g.*, rice husk ash [134,135]) or diatomaceous
405 earth [136] as SCMs. One study evaluated the pozzolanic reactivity of biosilica harvested from
406 freshly cultured diatoms (*i.e.*, *Thalassiosira pseudonana* and *Phaeodactylum tricornutum*) in
407 accordance with ASTM C1897 [31]. Aside from metakaolin, diatom biosilica extracted from *T.*
408 *pseudonana* exhibited the highest bound water content (9.9 ± 0.6 g/100 g dried paste), indicating
409 high pozzolanic reactivity. Contrastingly, diatom biosilica extracted from *P. tricornutum* was less
410 reactive (4.3 ± 0.1 g/100 g dried paste) but exhibited similar pozzolanic reactivity to a Class F fly

411 ash. Overall, the data highlighted the potential to grow reactive biominerals for use as alternative
412 SCMs using CO₂-sequestering microorganisms.
413

414 **4.3 Emerging Applications, Opportunities, and Challenges**

415 In addition to the previous examples, biomineralized CaCO₃ and SiO₂ have other potential uses
416 within cement and concrete field. For example, biomineralized CaCO₃ and SiO₂ could be used to
417 replace raw meal in portland cement production. The use of photosynthetic production of CO₂-
418 storing, biomineralized CaCO₃ as a limestone replacement could theoretically reduce the
419 embodied carbon emissions of portland cement manufacturing. Biomineralized SiO₂ from diatoms
420 could also be used to replace the silica provided by clays and sand during cement production. To
421 produce the CaCO₃ or SiO₂ in a photosynthetic manner, cement producers would need access to
422 seawater and CO₂. The potential use of CO₂ waste streams (e.g., flue gas) from cement
423 manufacturing for microorganism growth is an advantage of this approach.

424 Microorganisms can produce nanoscale CaCO₃ and SiO₂, rendering these particles
425 excellent candidates as reactive additives to cementitious systems [80]. The reactivity of these
426 particles could be tailored by physically or genetically modulating the biomineralization process.
427 For example, CaCO₃ could be rendered more reactive by targeting the formation and stabilization
428 of more reactive CaCO₃ polymorphs (*i.e.*, vaterite, aragonite, ACC) or more intricate morphologies
429 (*i.e.*, higher surface area). The chemical composition of biomineralized SiO₂ extracted from
430 diatoms could be modified to include other beneficial metal cations (e.g., Al, Fe) through doping
431 of the culture media. To that end, biomineralized SiO₂ could also be used in the production of
432 sodium silicate (*i.e.*, waterglass) that is necessary for alkali activation or, if doped with Al, reactive
433 precursors for alkali-activated cements.

434 The use of enzymes to produce biomineralized cementitious materials is an emerging area
435 of high-impact scientific research. Enzyme-based mineralization has several advantages over
436 conventional biomineralization mechanisms, including fewer resources that are otherwise required
437 for full-scale growth. As evidenced by the work with urea [34,38] and some emerging work with
438 carbonic anhydrase [34,137], the enzymes need only be present in small quantities to achieve
439 similar degrees of mineralization to systems containing the living microorganisms. Conversely,
440 the exact inhibition effects of cement pore solution and other additives on the catalytic behavior
441 of enzymes are not fully understood and require further investigation [52].

442 As with any novel material technology, there are several challenges to consider in regard
443 to widespread implementation of CaCO₃ and SiO₂ biomineralization. First, at-scale cost and scale
444 of production is a key consideration. One promising aspect is that the global capacity of oceanic
445 CaCO₃ is estimated to be 5.48 billion metric tons [138,139], and biogenic SiO₂ from surface ocean
446 would be estimated to be 14 billion metric tons [140]. The cost of scaling the production of
447 biomineralized CaCO₃ and SiO₂ will differ by biomineralization mechanism and organism species.
448 To that end, photosynthesis-driven CaCO₃ and SiO₂ biomineralization have a cost advantage over
449 other biomineralization mechanisms, given that the energy and material inputs (e.g., sunlight,
450 seawater) are abundantly available. At-scale production cost of biomineralized CaCO₃ and SiO₂
451 could be further ameliorated through the valorization of organic byproducts (*i.e.*, lipids, proteins,
452 carbohydrates), which may have applications in biofuels [75], catalysis [7], and medicine [141].
453 In addition to cost, elucidating the effects of new biominerals on fresh- and hardened-state
454 properties of cementitious materials is a key technical challenge. This challenge is particularly
455 relevant to new material systems (e.g., enzyme-based building materials) whose long-term
456 durability needs to be understood prior to widespread implementation. Finally, shifting paradigms

457 within the cement and concrete industry from one historically rooted in mining and extraction of
458 minerals to one centered on cultivation (*i.e.*, farming) of minerals remains a barrier but one that
459 perhaps soon will be overcome in light of the current climate crisis and a steady global shift toward
460 fully regenerative practices.

461

462 **5.0 Conclusions**

463 Biominerization is an emerging area of interest within the field of cement and concrete research.
464 In this work, the mechanisms of CaCO_3 and SiO_2 biominerization were reviewed, and the
465 morphological diversity of CaCO_3 and SiO_2 architectures were highlighted and discussed. In
466 addition, this work reviewed traditional applications of CaCO_3 and SiO_2 biominerization in
467 cement and concrete research, including self-healing, self-sealing, soil stabilization, and recycled
468 aggregate beneficiation, along with emerging applications, such as biominerized CaCO_3 fillers
469 in cementitious materials and the production of living and enzymatically mineralized construction
470 materials. Potentially new application areas of CaCO_3 and SiO_2 biominerization were
471 highlighted, including the use of CaCO_3 and SiO_2 as the raw materials for portland cement, SCM,
472 and alkali-activated cement production. Finally, this work addressed the challenges and barriers to
473 implementing new material technologies in the field, such as cost and scale of production, as well
474 as the technical, regulatory, and perception barriers that must be addressed prior to widespread
475 implementation.

476

477 **6.0 Acknowledgments**

478 This research was supported by the Department of Civil, Environmental, and Architectural
479 Engineering, the Materials Science and Engineering Program, and the Living Materials Laboratory
480 at the University of Colorado Boulder, with financial support from the United States (US) National
481 Science Foundation (Grant No. CMMI-1943554). The authors gratefully acknowledge Danielle
482 Beatty, Dr. Cansu Acarturk, and Dr. Caitlin Adams for their insightful comments. This work
483 represents the views of the authors and does not necessarily reflect the position or the policy of the
484 US Government.

485

486 **7.0 Disclosures**

487 WVS is listed as a co-inventor on a patent application PCT/US2020/020863 and
488 PCT/US2020/058344 filed by the University of Colorado. WVS is a co-founder and shareholder
489 of Prometheus Materials, Inc. and Minus Materials, Inc. and a member of their advisory boards.

490

491 **8.0 Authorship Statement (CRediT)**

492 Nicolas D. Dowdy: Conceptualization, Investigation, Writing-original draft, Writing-reviewing
493 and editing, Visualization. Wil V. Srubar III: Conceptualization, Writing-original draft, Writing-
494 reviewing and editing, Supervision, Visualization, Project administration, Funding acquisition.

495

496

497

498 **8.0 References**

499 [1] S. Weiner, and P. M. Dove, An Overview of Biominerization Processes and the Problem
500 of the Vital Effect. *Reviews in Mineralogy and Geochemistry* (2003) 54(1): 1–29.

501 [2] M. Nodehi, T. Ozbakkaloglu, and A. Gholampour, A systematic review of bacteria-based
502 self-healing concrete: Biomineralization, mechanical, and durability properties. *Journal of*
503 *Building Engineering* (2022) 49: 104038.

504 [3] J. Zhao, L. Csetenyi, and G. M. Gadd, Fungal-induced CaCO₃ and SrCO₃ precipitation:
505 a potential strategy for bioprotection of concrete. *Science of The Total Environment* (2022) 816:
506 151501.

507 [4] I. Jakob, M. A. Chairopoulou, M. Vučak, C. Posten, and U. Teipel, Biogenic calcite
508 particles from microalgae—Coccoliths as a potential raw material. *Eng Life Sci* (2017) 17(6):
509 605–612.

510 [5] L. Addadi, D. Joester, F. Nudelman, and S. Weiner, Mollusk Shell Formation: A Source of
511 New Concepts for Understanding Biomineralization Processes. *Chem. Eur. J.* (2006) 12(4): 980–
512 987.

513 [6] T. M. DeCarlo, M. Holcomb, and M. T. McCulloch, Reviews and syntheses: Revisiting
514 the boron systematics of aragonite and their application to coral calcification. *Biogeosciences*
515 (2018) 15(9): 2819–2834.

516 [7] L. Köhler, S. Machill, A. Werner, C. Selzer, S. Kaskel, and E. Brunner, Are Diatoms
517 “Green” Aluminosilicate Synthesis Microreactors for Future Catalyst Production? *Molecules*
518 (2017) 22(12): 2232.

519 [8] S. M. La Vars, M. R. Johnston, J. Hayles, J. R. Gascooke, M. H. Brown, S. C. Leterme, et
520 al., ²⁹Si{¹H} CP-MAS NMR comparison and ATR-FTIR spectroscopic analysis of the diatoms
521 *Chaetoceros muelleri* and *Thalassiosira pseudonana* grown at different salinities. *Anal Bioanal
522 Chem* (2013) 405(10): 3359–3365.

523 [9] M. Sumper, and E. Brunner, Silica Biomineralisation in Diatoms: The Model Organism
524 *Thalassiosira pseudonana*. *ChemBioChem* (2008) 9(8): 1187–1194.

525 [10] K. Singh, M. Krishna Paidi, A. Kulshrestha, P. Bharmoria, S. Kumar Mandal, and A.
526 Kumar, Deep eutectic solvents based biorefining of Value-added chemicals from the diatom
527 *Thalassiosira andamanica* at room temperature. *Separation and Purification Technology* (2022)
528 298: 121636.

529 [11] O. Vinn, Phosphatic Biomineralization in Scyphozoa (Cnidaria): A Review. *Minerals*
530 (2022) 12(10): 1316.

531 [12] S. J. Omelon, and M. D. Grynpas, Relationships between Polyphosphate Chemistry,
532 Biochemistry and Apatite Biomineralization. *Chem. Rev.* (2008) 108(11): 4694–4715.

533 [13] J. P. Gevaudan, Z. Craun, and W. V. Srubar, Sulfuric acid degradation of alkali-activated
534 metakaolin cements supplemented with brucite. *Cement and Concrete Composites* (2021) 121:
535 104063.

536 [14] B. Tesson, C. Gaillard, and V. Martin-Jézéquel, Brucite formation mediated by the diatom
537 *Phaeodactylum tricornutum*. *Marine Chemistry* (2008) 109(1–2): 60–76.

538 [15] P. Yuan, D. Liu, J. Zhou, Q. Tian, Y. Song, H. Wei, et al., Identification of the occurrence
539 of minor elements in the structure of diatomaceous opal using FIB and TEM-EDS. *American
540 Mineralogist* (2019) 104(9): 1323–1335.

541 [16] K. Zeth, E. Hoiczyk, and M. Okuda, Ferroxidase-Mediated Iron Oxide Biomineralization:
542 Novel Pathways to Multifunctional Nanoparticles. *Trends in Biochemical Sciences* (2016) 41(2):
543 190–203.

544 [17] P. He, J. Guo, L. Lei, J. Jiang, Q. Li, Z. Hu, et al., *Escherichia coli* templated iron oxide
545 biomineralization under oscillation. *RSC Advances* (2021) 11(25): 15010–15016.

546 [18] L. Zhou, F. Liu, Q. Liu, C. Fortin, Y. Tan, L. Huang, et al., Aluminum increases net
547 carbon fixation by marine diatoms and decreases their decomposition: Evidence for the iron–
548 aluminum hypothesis. *Limnol Oceanogr* (2021) 66(7): 2712–2727.

549 [19] S. Machill, L. Köhler, S. Ueberlein, R. Hedrich, M. Kunaschk, S. Paasch, et al.,
550 Analytical studies on the incorporation of aluminium in the cell walls of the marine diatom
551 *Stephanopyxis turris*. *Biometals* (2013) 26(1): 141–150.

552 [20] E. Trembath-Reichert, J. P. Wilson, S. E. McGlynn, and W. W. Fischer, Four hundred
553 million years of silica biomineralization in land plants. *Proceedings of the National Academy of
554 Sciences* (2015) 112(17): 5449–5454.

555 [21] S. Omelon, J. Georgiou, F. Variola, and M. N. Dean, Colocation and role of
556 polyphosphates and alkaline phosphatase in apatite biomineralization of elasmobranch tesserae.
557 *Acta Biomaterialia* (2014) 10(9): 3899–3910.

558 [22] S. Chakraborty, S. Bag, S. Pal, and A. K. Mukherjee, Structural and microstructural
559 characterization of bioapatites and synthetic hydroxyapatite using X-ray powder diffraction and
560 Fourier transform infrared techniques. *J Appl Cryst* (2006) 39(3): 385–390.

561 [23] M. Wysokowski, T. Jasionowski, and H. Ehrlich, Biosilica as a source for inspiration in
562 biological materials science. *American Mineralogist* (2018) 103(5): 665–691.

563 [24] S. Marín, O. Cabestrero, C. Demergasso, S. Olivares, V. Zetola, and M. Vera, An
564 indigenous bacterium with enhanced performance of microbially-induced Ca-carbonate
565 biomineralization under extreme alkaline conditions for concrete and soil-improvement
566 industries. *Acta Biomaterialia* (2021) 120: 304–317.

567 [25] S. Kenai, Recycled aggregates. *Waste and Supplementary Cementitious Materials in
568 Concrete*. Elsevier, 2018, 79–120.

569 [26] R. H. Faraj, A. A. Mohammed, K. M. Omer, and H. U. Ahmed, Soft computing
570 techniques to predict the compressive strength of green self-compacting concrete incorporating
571 recycled plastic aggregates and industrial waste ashes. *Clean Techn Environ Policy* (2022) 24(7):
572 2253–2281.

573 [27] M.-G. Ma, F. Deng, K. Yao, and C.-H. Tian, Microwave-assisted Synthesis and
574 Characterization of CaCO₃ Particles-filled Wood Powder Nanocomposites. *BioResources* (2014)
575 9.

576 [28] H.-J. Chen, H.-L. Chang, C.-W. Tang, and T.-Y. Yang, Application of Biomineralization
577 Technology to Self-Healing of Fiber-Reinforced Lightweight Concrete after Exposure to High
578 Temperatures. *Materials* (2022) 15(21): 7796.

579 [29] H. Hermawan, A. Simons, S. Teirlynck, P. Serna, P. Minne, G. Anglani, et al.,
580 Applicability of cementitious capsules in concrete production: initial assessment on capsule
581 robustness, mechanical and self-sealing properties of concrete. *MATEC Web Conf.* (2023) 378:
582 02013.

583 [30] B. Park, and Y. C. Choi, Evaluation of crack self-sealing in flexural concrete members
584 with SAPs by chloride ion penetration resistance. *Journal of Building Engineering* (2023) 76:
585 107132.

586 [31] S. L. Williams, Use of Siliceous and Calcareous Microalgae to Decarbonize Cement
587 Production / Sarah Lynn Williams. *Dissertations Abstracts International* (2022) 84–03B.

588 [32] C. M. Heveran, L. Liang, A. Nagarajan, M. H. Hubler, R. Gill, J. C. Cameron, et al.,
589 Engineered Ureolytic Microorganisms Can Tailor the Morphology and Nanomechanical
590 Properties of Microbial-Precipitated Calcium Carbonate. *Sci Rep* (2019) 9(1): 14721.

591 [33] L. Liang, R. Liu, K. E. O. Foster, AlakshChoudhury, S. Cook, J. C. Cameron, et al.,
592 Genome engineering of *E. coli* for improved styrene production. *Metabolic Engineering* (2020)
593 57: 74–84.

594 [34] M. Tepe, Ş. Arslan, T. Koralay, and N. Mercan Doğan, Precipitation and characterization
595 of CaCO_3 of *Bacillus amyloliquefaciens* U17 strain producing urease and carbonic anhydrase.
596 *Turk J Biol* (2019) 43(3): 198–208.

597 [35] R. Rautela, and S. Rawat, Analysis and optimization of process parameters for *in vitro*
598 biomineralization of CaCO_3 by *Klebsiella pneumoniae*, isolated from a stalactite from the
599 Sahastradhara cave. *RSC Adv.* (2020) 10(14): 8470–8479.

600 [36] B. M. Kirpat Konak, M. E. Bakar, R. E. Ahan, E. U. Özyürek, S. Dökmeci, and U. Ö.
601 Şafak Şeker, A living material platform for the biomineralization of biosilica. *Materials Today*
602 *Bio* (2022) 17: 100461.

603 [37] W. Qin, C. Wang, Y. Ma, M. Shen, J. Li, K. Jiao, et al., Microbe-Mediated Extracellular
604 and Intracellular Mineralization: Environmental, Industrial, and Biotechnological Applications.
605 *Advanced Materials* (2020) 32(22): 1907833.

606 [38] B. Krajewska, Urease-aided calcium carbonate mineralization for engineering
607 applications: A review, *Journal of Advanced Research* (2018) 13: 59–67.

608 [39] S. Wei, H. Cui, Z. Jiang, H. Liu, H. He, and N. Fang, Biomineralization processes of
609 calcite induced by bacteria isolated from marine sediments. *Braz. J. Microbiol.* (2015) 46(2):
610 455–464.

611 [40] G. Neukermans and G. Fournier, An analytical model for light backscattering by
612 coccoliths and coccospores of *Emiliania huxleyi*. *Optics Express* (2018) 25(13): 14996.

613 [41] X. Chen, A. K. S. Kameshwar, C. Chio, F. Lu, W. Qin, Effect of KNO_3 on Lipid
614 Synthesis and CaCO_3 Accumulation in *Pleurochrysis dentata* coccoliths with a Special Focus on
615 Morphological Characters of Coccolithophores, *International Journal of Biological Sciences*
616 (2019) 15(13): 2844–2858.

617 [42] C. Y. Lin, A. V. Turchyn, Z. Steiner, P. Bots, G. I. Lampronti, and N. J. Tosca, The role of
618 microbial sulfate reduction in calcium carbonate polymorph selection. *Geochimica et*
619 *Cosmochimica Acta* (2018) 237: 184–204.

620 [43] S. Huang, X. Zhang, Y. Song, G. He, Z. Wang, B. Lian, Bio-mineralisation,
621 characterization, and stability of calcium carbonate containing organic matter. *RSC Adv.* (2021)
622 11(24): 14415–14425.

623 [44] G. Grellet-Tinner, L. E. Fiorelli, and R. B. Salvador, Water Vapor Conductance Of The
624 Lower Cretaceous Dinosaurian Eggs From Sanagasta, La Rioja, Argentina: Paleobiological And
625 Paleoecological Implications For South American Faveoloolithid And Megaloolithid Eggs.
626 *Palaios* (2012) 27 (1): 35–47.

627 [45] A. Periasamy, C.-H. Kang, Y.-J. Shin, J.-S. So, Formations of calcium carbonate minerals
628 by bacteria and its multiple applications (2016) 5 (1): 250.

629 [46] M. Tepe, S. Arslan, T. Koralay, N. Mercan Dogan, Precipitation and characterization of
630 CaCO_3 of *Bacillus amyloliquefaciens* U17 strain producing urease and carbonic anhydrase
631 (2019) 43 (3): 198–208.

632 [47] D. N. Beatty, S. L. Williams, and W. V. Srubar, Biomineralized Materials for Sustainable
633 and Durable Construction. *Annu. Rev. Mater. Res.* (2022) 52(1): 411–439.

634 [48] C. Jansson, and T. Northen, Calcifying cyanobacteria—the potential of biomineralization
635 for carbon capture and storage. *Current Opinion in Biotechnology* (2010) 21(3): 365–371.

636 [49] C. McNicholl, and M. S. Koch, Irradiance, photosynthesis and elevated pCO₂ effects on
637 net calcification in tropical reef macroalgae. *Journal of Experimental Marine Biology and*
638 *Ecology* (2021) 535: 151489.

639 [50] C. J. Daniels, A. J. Poulton, W. M. Balch, E. Marañón, T. Adey, B. C. Bowler, et al., A
640 global compilation of coccolithophore calcification rates. *Earth System Science Data* (2018)
641 10(4): 1859–1876.

642 [51] V. Achal, A. Mukherjee, D. Kumari, and Q. Zhang, Biominerization for sustainable
643 construction – A review of processes and applications. *Earth-Science Reviews* (2015) 148: 1–17.

644 [52] C. Rodriguez-Navarro, Ö. Cizer, K. Kudłacz, A. Ibañez-Velasco, C. Ruiz-Agudo, K.
645 Elert, et al., The multiple roles of carbonic anhydrase in calcium carbonate mineralization.
646 *CrystEngComm* (2019) 21(48): 7407–7423.

647 [53] M. C. Murphy, D. N. Beatty, and W. V. Srb, Structure and Properties of Portland-
648 Limestone Cements Synthesized with Biologically Architected Calcium Carbonate. *Bio-Based*
649 *Building Materials*, S. Amziane, I. Merta, and J. Page (Eds.), Switzerland (Cham) 21–23 June
650 2023, Springer Nature Switzerland, 2023, 42–53.

651 [54] S. Wang, S. F. Scarlata, and N. Rahbar, A self-healing enzymatic construction material.
652 *Matter* (2022) 5(3): 957–974.

653 [55] S. C. Chuo, S. F. Mohamed, S. H. Mohd Setapar, A. Ahmad, M. Jawaid, W. A. Wani, et
654 al., Insights into the Current Trends in the Utilization of Bacteria for Microbially Induced
655 Calcium Carbonate Precipitation. *Materials* (2020) 13(21): 4993.

656 [56] P. Gao, and K. Fan, Sulfur-oxidizing bacteria (SOB) and sulfate-reducing bacteria (SRB)
657 in oil reservoir and biological control of SRB: a review. *Arch Microbiol* (2023) 205(5): 162.

658 [57] Z. Zhang, C. Zhang, Y. Yang, Z. Zhang, Y. Tang, P. Su, et al., A review of sulfate-
659 reducing bacteria: Metabolism, influencing factors and application in wastewater treatment.
660 *Journal of Cleaner Production* (2022) 376: 134109.

661 [58] T. Bosak, and D. K. Newman, Microbial nucleation of calcium carbonate in the
662 Precambrian. *Geol* (2003) 31(7): 577.

663 [59] K. Janssen, B. Mähler, J. Rust, G. Bierbaum, and V. E. McCoy, The complex role of
664 microbial metabolic activity in fossilization. *Biological Reviews* (2022) 97(2): 449–465.

665 [60] A. F. Alshalif, J. M. Irwan, N. Othman, and L. H. Anneza, Isolation of Sulphate
666 Reduction Bacteria (SRB) to Improve Compress Strength and Water Penetration of Bio-
667 Concrete. *MATEC Web of Conferences* (2016) 47: 01016.

668 [61] D. C. Bassett, M. D. McKee, and J. E. Barralet, The Role of the Air–Liquid Interface in
669 Protein-Mediated Biominerization of Calcium Carbonate. *Crystal Growth & Design* (2011)
670 11(3): 803–810.

671 [62] R. Sandya Rani, and M. Saharay, Molecular dynamics simulation of protein-mediated
672 biominerization of amorphous calcium carbonate. *RSC Advances* (2019) 9(3): 1653–1663.

673 [63] C. Briegel, J. Seto, Single Amino Acids as Additives Modulating CaCO₃ Mineralization
674 (*Advanced Topics in Biominerization*).

675 [64] X. Wang, R. Kong, X. Pan, H. Xu, D. Xia, H. Shan, J. R. Lu, Role of Ovalbumin in the
676 Stabilization of Metastable Vaterite in Calcium Carbonate Biominerization (2009) 113(26):
677 8975–8982.

678 [65] I. Polowczyk, A. Bastryzk, M. Fiedot, Protein-Mediated Precipitation of Calcium
679 Carbonate (2016) 9(11): 944.

680 [66] W. R. Francis, M. Eitel, S. Vargas, C. A. Garcia-Escudero, N. Conci, F. Deister, et al., The
681 genome of the reef-building glass sponge *Aphrocallistes vastus* provides insights into silica
682 biomineralization. *R. Soc. Open Sci.* (2023) 10(6): 230423.

683 [67] J. E. Dove, C. M. Shillaber, T. S. Becker, A. F. Wallace, and P. M. Dove, Biologically
684 Inspired Silicification Process for Improving Mechanical Properties of Sand. *J. Geotech.*
685 *Geoenviron. Eng.* (2011) 137(10): 949–957.

686 [68] G. Taveri, S. Grasso, F. Gucci, J. Toušek, and I. Dlouhy, Bio-Inspired Hydro-Pressure
687 Consolidation of Silica. *Advanced Functional Materials* (2018) 28: 1805794.

688 [69] S. Imbler, *A Swirling Vortex Is No Match for This Deep-Sea Sponge*, *The New York Times*
689 (2021).

690 [70] M. A. Monn, Learning new tricks from sea sponges, nature's most unlikely civil
691 engineers, available at <https://phys.org/news/2017-08-sea-sponges-nature-civil.html>.

692 [71] C. C. Piccinetti, R. Ricci, C. Pennesi, G. Radaelli, C. Totti, et al., Herbivory in the soft
693 coral *Sinularia flexibilis* (Alcyoniidae). *Scientific Reports* (2016) 6(1): 22679

694 [72] P. G. Falkowski, and J. A. Raven, *Aquatic Photosynthesis*: Second Edition, Princeton
695 University Press, 2013.

696 [73] E. Koning, M. Gehlen, A.-M. Flank, G. Calas, and E. Epping, Rapid post-mortem
697 incorporation of aluminum in diatom frustules: Evidence from chemical and structural analyses.
698 *Marine Chemistry* (2007) 106(1–2): 208–222.

699 [74] W.-X. Wang, and R. C. H. Dei, Metal uptake in a coastal diatom influenced by major
700 nutrients (N, P, and Si). *Water Research* (2001) 35(1): 315–321.

701 [75] H. Jin, H. Zhang, Z. Zhou, K. Li, G. Hou, Q. Xu, et al., Ultrahigh-cell-density
702 heterotrophic cultivation of the unicellular green microalga *Scenedesmus acuminatus* and
703 application of the cells to photoautotrophic culture enhance biomass and lipid production.
704 *Biotechnology and Bioengineering* (2020) 117(1): 96–108.

705 [76] Limestone | Characteristics, Formation, Texture, Uses, & Facts | Britannica, available at
706 <https://www.britannica.com/science/limestone>.

707 [77] B. Jones, Review of calcium carbonate polymorph precipitation in spring systems.
708 *Sedimentary Geology* (2017) 353: 64–75.

709 [78] O. Cherkas, T. Beuvier, F. Zontone, Y. Chushkin, L. Demoulin, A. Rousseau, A. Gibaud,
710 On the kinetics of phase transformations of dried porous vaterite particles immersed in deionized
711 and tap water (2018) 29(11): 2872–2880.

712 [79] N. Mehta, J. Gaëtan, P. Giura, T. Azaïs, and K. Benzerara, Detection of biogenic
713 amorphous calcium carbonate (ACC) formed by bacteria using FTIR spectroscopy.
714 *Spectrochimica Acta Part A: Molecular and Biomolecular Spectroscopy* (2022) 278: 121262.

715 [80] D. Zhao, J. M. Williams, Z. Li, A.-H. A. Park, A. Radlińska, P. Hou, et al., Hydration of
716 cement pastes with calcium carbonate polymorphs. *Cement and Concrete Research* (2023) 173:
717 107270.

718 [81] T. Yang, R. He, G. Nie, W. Wang, G. Zhang, Y. Hu, et al., Creation of Hollow Calcite
719 Single Crystals with CQDs: Synthesis, Characterization, and Fast and Efficient Decontamination
720 of Cd(II). *Sci Rep* (2018) 8(1): 17603.

721 [82] H. Gilad, H. Barhum, A. Ushkov, A. Machnev, D. Ofer, V. Bobrovs, et al., Gilded vaterite
722 optothermal transport in a bubble. *Sci Rep* (2023) 13(1): 12158.

723 [83] B. Myszka, M. Schüßler, K. Hurle, B. Demmert, R. Detsch, et al., Phase-specific
724 bioactivity and altered Ostwald ripening pathways of calcium carbonate polymorphs in simulated
725 body fluid. *RSC Advances* (2019) 9(32): 18232–18244.

726 [84] J. M. Xto, C. N. Borca, J. A. van Bokhoven, T. Huthwelker, Aerosol-based synthesis of
727 pure and stable amorphous calcium carbonate. *Chemical Communications* (2019) 55(72): 10725-
728 10728.

729 [85] Calcite | mineral | Britannica, available at <https://www.britannica.com/science/calcite>.

730 [86] B. Suchéras-Marx, S. Viseur, C. E. Walker, L. Beaufort, I. Probert, and C. Bolton,
731 Coccolith size rules – What controls the size of coccoliths during coccolithogenesis? *Marine
732 Micropaleontology* (2022) 170: 102080.

733 [87] F. Neuweiler, S. Kershaw, F. Boulvain, M. Matysik, C. Sendino, M. McMenamin, et al.,
734 Keratose sponges in ancient carbonates – A problem of interpretation. *Sedimentology* (2023)
735 70(3): 927–968.

736 [88] M. Sancho-Tomás, S. Fermani, J. Gómez-Morales, G. Falini, and J. Garcia-Ruiz,
737 Calcium carbonate bio-precipitation in counter-diffusion systems using the soluble organic
738 matrix from nacre and sea-urchin spine. *European Journal of Mineralogy* (2014) 26.

739 [89] X. Jin, W. Ma, and C. Liu, Origin of the long-term increase in coccolith size and its
740 implication for carbon cycle and climate over the past 2 Myr. *Quaternary Science Reviews*
741 (2022) 290: 107642.

742 [90] B. Myszka, M. Schüßler, K. Hurle, B. Demmert, R. Detsch, A. R. Boccaccini, et al.,
743 Phase-specific bioactivity and altered Ostwald ripening pathways of calcium carbonate
744 polymorphs in simulated body fluid. *RSC Adv.* (2019) 9(32): 18232–18244.

745 [91] Y. Ma, Q. Feng, and X. Bourrat, A novel growth process of calcium carbonate crystals in
746 silk fibroin hydrogel system. *Materials Science and Engineering: C* (2013) 33(4): 2413–2420.

747 [92] M. He, Y. Cai, H. Zhang, G. Xue, X. Cheng, Y. Lu, et al., The impact and implications of
748 aragonite-to-calcite transformation on speleothem trace element composition. *Sedimentary
749 Geology* (2021) 425: 106010.

750 [93] B. C. Chakoumakos, B. M. Pracheil, R. P. Koenigs, R. M. Bruch, and M. Feygenson,
751 Empirically testing vaterite structural models using neutron diffraction and thermal analysis. *Sci
752 Rep* (2016) 6: 36799.

753 [94] H. A. Lowenstam, and D. P. Abbott, Vaterite: A Mineralization Product of the Hard
754 Tissues of a Marine Organism (Asciidiacea). *Science* (1975) 188(4186): 363–365.

755 [95] S. E. Grasby, Naturally precipitating vaterite (μ -CaCO₃) spheres: unusual carbonates
756 formed in an extreme environment. *Geochimica et Cosmochimica Acta* (2003) 67(9): 1659–
757 1666.

758 [96] L. Yi, B. Zou, L. Xie, and R. Zhang, A novel bifunctional protein PNU7 in CaCO₃
759 polymorph formation: Vaterite stabilization and surface energy minimization. *International
760 Journal of Biological Macromolecules* (2022) 222: 2796–2807.

761 [97] R. Liu, S. Huang, X. Zhang, Y. Song, G. He, Z. Wang, et al., Bio-mineralisation,
762 characterization, and stability of calcium carbonate containing organic matter. *RSC Adv.* (2021)
763 11(24): 14415–14425.

764 [98] D. B. Trushina, T. V. Bukreeva, M. V. Kovalchuk, and M. N. Antipina, CaCO₃ vaterite
765 microparticles for biomedical and personal care applications. *Materials Science and Engineering:
766 C* (2014) 45: 644–658.

767 [99] H. Choi, H. Choi, M. Inoue, and R. Sengoku, Control of the Polymorphism of Calcium
768 Carbonate Produced by Self-Healing in the Cracked Part of Cementitious Materials. *Applied
769 Sciences* (2017) 7(6): 546.

770 [100] I. Segovia-Campos, A. Martignier, M. Filella, J. Jaquet, and D. Ariztegui, Micropearls
771 and other intracellular inclusions of amorphous calcium carbonate: an unsuspected

772 biomineralization capacity shared by diverse microorganisms. *Environmental Microbiology*
773 (2022) 24(2): 537–550.

774 [101] M. Farhadi Khouzani, D. M. Chevrier, P. Gütlein, K. Hauser, P. Zhang, N. Hedin, et al.,
775 Disordered amorphous calcium carbonate from direct precipitation. *CrystEngComm* (2015)
776 17(26): 4842–4849.

777 [102] X. Xu, J. T. Han, and K. Cho, Formation of Amorphous Calcium Carbonate Thin Films
778 and Their Role in Biomineralization. *Chem. Mater.* (2004) 16(9): 1740–1746.

779 [103] Ye. V. Likhoshway, E. G. Sorokovikova, O. I. Belykh, O. L. V. Kaluzhnaya, S. I. Belikov,
780 Ye. D. Bedoshvili, et al., Visualization of the Silicon Biomineralization in Cyanobacteria,
781 Sponges and Diatoms, in *Biosphere Origin and Evolution*, eds. Dobretsov, N., Kolchanov, N.,
782 Rozanov, A., and Zavarzin, G., (Springer US, Boston, MA, 2008), pp. 219–230.

783 [104] W. E. G. Müller, H. C. Schröder, U. Schlossmacher, M. Neufurth, W. Geurtsen, M.
784 Korzhev, et al., The enzyme carbonic anhydrase as an integral component of biogenic Ca-
785 carbonate formation in sponge spicules. *FEBS Open Bio* (2013) 3(1): 357–362.

786 [105] C. Heintze, I. Babenko, J. Zackova Suchanova, A. Skeffington, B. M. Friedrich, and N.
787 Kröger, The molecular basis for pore pattern morphogenesis in diatom silica. *Proc Natl Acad Sci
788 U S A* (2022) 119(49): e2211549119.

789 [106] M. L. Gillmore, L. A. Golding, B. M. Angel, M. S. Adams, and D. F. Jolley, Toxicity of
790 dissolved and precipitated aluminium to marine diatoms. *Aquatic Toxicology* (2016) 174: 82–91.

791 [107] Y. Wang, D. Zhang, J. Pan, and J. Cai, Key factors influencing the optical detection of
792 biomolecules by their evaporative assembly on diatom frustules. *J Mater Sci* (2012) 47(17):
793 6315–6325.

794 [108] D. Zhang, Y. Wang, W. Zhang, J. Pan, and J. Cai, Enlargement of diatom frustules pores
795 by hydrofluoric acid etching at room temperature. *J Mater Sci* (2011) 46(17): 5665–5671.

796 [109] G. L Rorrer, and A. X Wang, Nanostructured diatom frustule immunosensors. *Front
797 Nanosci Nanotech* (2016) 2(3): 128-130.

798 [110] I. Zgłobicka, and K. J. Kurzydłowski, Multi-length scale characterization of frustule
799 showing highly hierachal structure in the context of understanding their mechanical properties.
800 *Materials Today Communications* (2022) 33: 104741.

801 [111] M. Hildebrand, Diatoms, Biomineralization Processes, and Genomics. *Chem. Rev.* (2008)
802 108(11): 4855–4874.

803 [112] K. Leblanc, B. Quéguiner, F. Diaz, V. Cornet, M. Michel-Rodriguez, X. Durrieu de
804 Madron, et al., Nanoplanktonic diatoms are globally overlooked but play a role in spring blooms
805 and carbon export. *Nat Commun* (2018) 9(1): 953.

806 [113] N. K. Dhami, M. S. Reddy, and A. Mukherjee, Biomineralization of calcium carbonates
807 and their engineered applications: a review. *Front. Microbiol.* (2013) 4.

808 [114] L. Tan, J. Xu, Y. Wei, and W. Yao, The effect of bacteria *Bacillus Cohnii* on the
809 synthesised calcium silicate hydrate (C–S–H) with various calcium to silica ratio in nanoscale.
810 *Cement and Concrete Composites* (2022) 134: 104779.

811 [115] A. M. Grabiec, J. Klama, D. Zawal, and D. Krupa, Modification of recycled concrete
812 aggregate by calcium carbonate biodeposition. *Construction and Building Materials* (2012) 34:
813 145–150.

814 [116] M. A. Bakr, and B. K. Singh, Effect of biomineralized *Bacillus subtilis* on recycled
815 aggregate concrete containing blended hydrated lime and brick powder. *Case Studies in
816 Construction Materials* (2023) 18: e02137.

817 [117] G. Moita, V. Liduino, E. F. Servulo, J. P. Bassin, and R. D. Toledo Filho, Isolation of
818 Bacterial Strains from Concrete Aggregates and Their Potential Application in Microbially
819 Induced Calcite Precipitation, in Bio-Based Building Materials, eds. Amziane, S., Merta, I., and
820 Page, J., (Springer Nature Switzerland, Cham, 2023), pp. 729–738.

821 [118] J. Qiu, J. Artier, S. Cook, W. V. Srbbar, J. C. Cameron, and M. H. Hubler, Engineering
822 living building materials for enhanced bacterial viability and mechanical properties. *IScience*
823 (2021) 24(2): 102083.

824 [119] S. A. Rizwan, H. Khan, T. A. Bier, and F. Adnan, Use of Effective Micro-organisms (EM)
825 technology and self-compacting concrete (SCC) technology improved the response of
826 cementitious systems. *Construction and Building Materials* (2017) 152: 642–650.

827 [120] C. M. Heveran, S. L. Williams, J. Qiu, J. Artier, M. H. Hubler, S. M. Cook, et al.,
828 Biomineralization and Successive Regeneration of Engineered Living Building Materials. *Matter*
829 (2020) 2(2): 481–494.

830 [121] N. Byrd, J. R. Lloyd, J. S. Small, F. Taylor, H. Bagshaw, C. Boothman, et al., Microbial
831 Degradation of Citric Acid in Low Level Radioactive Waste Disposal: Impact on
832 Biomineralization Reactions. *Frontiers in Microbiology* (2021) 12.

833 [122] L. Zhao, C. Cai, R. Jin, J. Li, H. Li, J. Wei, et al., Mineralogical and geochemical
834 evidence for biogenic and petroleum-related uranium mineralization in the Qianjiadian deposit,
835 NE China. *Ore Geology Reviews* (2018) 101: 273–292.

836 [123] R. Garg, R. Garg, and N. O. Eddy, Microbial induced calcite precipitation for self-healing
837 of concrete: a review. *Journal of Sustainable Cement-Based Materials* (2023) 12(3): 317–330.

838 [124] B. W. Chong, R. Othman, R. P. Jaya, X. Li, M. R. M. Hasan, and M. M. A. B. Abdullah,
839 Meta-analysis of studies on eggshell concrete using mixed regression and response surface
840 methodology. *Journal of King Saud University - Engineering Sciences* (2023) 35(4): 279–287.

841 [125] A. A. Jhatial, A. Kumar, N. Bheel, S. Sohu, and W. I. Goh, Assessing the sustainability
842 and cost-effectiveness of concrete incorporating various fineness of eggshell powder as
843 supplementary cementitious material. *Environ Sci Pollut Res* (2022) 29(56): 84814–84826.

844 [126] P. Nasaeng, A. Wongsa, R. Cheerarot, V. Sata, and P. Chindaprasirt, Strength
845 enhancement of pumice-based geopolymers paste by incorporating recycled concrete and calcined
846 oyster shell powders. *Case Studies in Construction Materials* (2022) 17: e01307.

847 [127] A. Bourdot, C. Martin-Cavaillé, M. Vacher, T. Honorio, N. Sebaibi, and R. Bennacer,
848 Microstructure and Durability Properties of Concretes Based on Oyster Shell Co-products, Proc.
849 of the 75th RILEM Annual Week 2021, J.I. Escalante-Garcia, P. Castro Borges, and A. Duran-
850 Herrera, Springer International Publishing, 2023, 65–73.

851 [128] B. Bunyamin, and A. Mukhlis, Utilization of Oyster Shells as a Substitute Part of Cement
852 and Fine Aggregate in the Compressive Strength of Concrete. *Aceh International Journal of*
853 *Science and Technology* (2020) 9(3): 150–156.

854 [129] I. Horiguchi, Y. Mimura, and P. J. M. Monteiro, Plant-growing performance of pervious
855 concrete containing crushed oyster shell aggregate. *Cleaner Materials* (2021) 2: 100027.

856 [130] B. A. Tayeh, M. W. Hasaniyah, A. M. Zeyad, and M. O. Yusuf, Properties of concrete
857 containing recycled seashells as cement partial replacement: A review. *Journal of Cleaner*
858 *Production* (2019) 237: 117723.

859 [131] H. M. Hamada, F. Abed, B. Tayeh, M. S. Al Jawahery, A. Majdi, and S. T. Yousif, Effect
860 of recycled seashells on concrete properties: A comprehensive review of the recent studies.
861 *Construction and Building Materials* (2023) 376: 131036.

862 [132] K. Martin, H. K. Tirkolaei, E. Kavazanjian, Enhancing the strength of granular material
863 with a modified enzyme-induced carbonate precipitation (EICP) treatment solution. *Construction*
864 and *Building Materials* (2021) 271: 121529

865 [133] E. Baffoe, A. Ghahremaninezhad, Effect of proteins on the mineralization, microstructure
866 and mechanical properties of carbonation cured calcium silicate. *Cement and Concrete*
867 *Composites* (2023) 141: 105121

868 [134] S. Kumar Das, A. Adediran, C. Rodrigue Kaze, S. Mohammed Mustakim, and N. Leklou,
869 Production, characteristics, and utilization of rice husk ash in alkali activated materials: An
870 overview of fresh and hardened state properties. *Construction and Building Materials* (2022)
871 345: 128341.

872 [135] B. Singh, Rice husk ash, in *Waste and Supplementary Cementitious Materials in*
873 *Concrete*, (Elsevier, 2018), pp. 417–460.

874 [136] E. Jud Sierra, S. A. Miller, A. R. Sakulich, K. MacKenzie, and M. W. Barsoum,
875 *Pozzolanic Activity of Diatomaceous Earth*. *Journal of the American Ceramic Society* (2010)
876 93(10):3406–3410.

877 [137] Worcester Polytechnic Inst Submits Patent Application for Chemical Analogs of Carbonic
878 Anhydrase for Concrete Repair. - Document - Gale OneFile: Business, available at
879 <https://go.gale.com/ps/i.do?p=ITBC&u=coloboulder&id=GALE%7CA744984840&v=2.1&it=r&sid=ebsco&aty=ip>.

880 [138] Seawater - Salinity, Biogeochemistry, and Trace Metals | Britannica (2023), available at
881 <https://www.britannica.com/science/seawater>, accessed July 5, 2023

882 [139] How Much Water is There on Earth? | U.S. Geological Survey.,
883 <https://www.usgs.gov/special-topics/water-science-school/science/how-much-water-there-earth#overview>, accessed July 5, 2023

884 [140] P. Tréguer, D. M. Nelson, A. J. Van Bennekom, D. J. DeMaster, A. Leynaert, B.
885 Quéguiner, The Silica Balance in the World Ocean: A Reestimate. *Science* (1995) 268(5209):
886 375-379.

887 [141] A. Noureddine, E. A. Hjelvik, J. G. Croissant, P. N. Durfee, J. O. Agola, and C. J.
888 Brinker, Engineering of large-pore lipid-coated mesoporous silica nanoparticles for dual cargo
889 delivery to cancer cells. *J Sol-Gel Sci Technol* (2019) 89(1) 78–90.